Environmental Engineering and Management Journal

October 2014, Vol.13, No. 10, 2675-2686
http://omicron.ch.tuiasi.ro/EEMJ/

"Gheorghe Asachi" Technical University of Iasi, Romania

REMOVAL OF CADMIUM (II) FROM AQUEOUS MEDIA USING COOH/TUD-1 MESOPOROUS SOLID. KINETIC AND THERMODYNAMIC STUDIES

Nabila Bensacia[1], Ioana Fechete[1*], Saâd Moulay[2], Saïda Debbih-Boustila[1], Anne Boos[3], François Garin[1]

[1]Institut de Chimie et Procédés pour l'Energie, l'Environnement et la Santé (ICPEES), UMR 7515 CNRS, Université de Strasbourg, 25 rue Becquerel, 67087, Strasbourg Cedex 2, France
[2]Laboratoire de Chimie-Physique Moléculaire et Macromoléculaire, Département de Chimie Industrielle, Faculté de Technologie, Université Saâd Dahlab de Blida, B. P. 270, Route de Soumâa, 09000, Blida, Algérie
[3]Institut Pluridisciplinaire Hubert Curien (IPHC), UMR 7178 CNRS, Université de Strasbourg, 25 rue Becquerel, 67087, Strasbourg Cedex 2, France

Abstract

The adsorption potential of 10 wt.% COOH/TUD-1 material for removing Cd^{2+} from aqueous solutions was investigated via the batch technique, and the effects of pH, temperature and contact time were studied. Experimental data showed that the maximum Cd^{2+} adsorption, 90%, occurred at pH 6. The adsorption equilibrium was reached within 35 min for 10 wt.% COOH/TUD-1. The adsorption mechanism was investigated in terms of its thermodynamics and kinetics. The adsorption data were fitted using the Langmuir and Freundlich isotherms, and the obtained modeling equilibrium adsorption data suggested that the 10 wt.% COOH/TUD-1 sample contained homogeneous adsorption sites that fit the Langmuir adsorption model well. The pseudo-second-order model described well the 10 wt.% COOH/TUD-1 adsorption process. The positive values of both $\Delta H°$ and $\Delta S°$ suggest, respectively, an endothermic reaction and an increase in randomness at the solid-liquid interface during the adsorption of Cd^{2+} onto the COOH/TUD-1 adsorbents. And, $\Delta G°$ values obtained were all negative, indicating a spontaneous adsorption process. Desorption and regeneration experiments indicated that ≈ 98% of the metals were desorbed. COOH/TUD-1 samples were characterized using N_2 adsorption-desorption isotherms, powder X-ray diffraction (XRD), Fourier-transform infrared (FT-IR) spectroscopy and Transmission electron microscopy (TEM).

Key words: adsorption, Cadmium, COOH/TUD-1, mesoporous sorbents

Received: February, 2014; Revised final: August, 2014; Accepted: August, 2014

1. Introduction

Since 1990, mesoporous silica obtained by the sol-gel process in the presence of a surfactant template (Beck et al., 1992; Beck and Vartuli, 1996) has attracted considerable attention from academic and industrial researchers (Bernal et al., 2012; Dumitriu et al., 2002; Fechete et al., 2012a; Hu et al., 2013; Visuvamithiran et al., 2013; Wu et al., 2013). After template removal, the mesoporous materials are characterized by large specific surface areas, narrow pore size distribution, free surface silanol groups and high thermal stability (Fechete et al., 2011; Staub et al., 2012; Tsoncheva et al., 2008). The internal surface of mesopore channels can be functionalized by covalent binding of suitable groups (-SH, -NH_2, -CN, -COOH). This can be accomplished either by post-synthesis grafting of a pre-formed mesoporous silica sample or via hydrolysis and co-condensation of inorganic silica precursors and silylated organic components (Da'na and Sayari, 2012; Delacôte et al., 2009; Ganesan and Walcarius, 2008; Jaber et al.,

∗ Author to whom all correspondence should be addressed: e-mail: ifechete@unistra.fr; Phone: +33 (0)3 68852737; Fax: +33 (0)368852761

2002a; Jaber et al., 2002b). Due to their intrinsic properties and to the possibilities for modifying them by introduction of active sites or by functionalization with suitable groups, mesoporous silicas stand as ideal materials for catalyst or catalyst support (Boulaoued et al., 2012; Fechete et al., 2012b, 2013; Ponomoreva et al., 2004; Tsoncheva et al., 2013), template for other materials (Sarshar et al., 2011; Yen et al., 2011), support for the immobilization of enzymes and other biologically active molecules (Dumitriu et al., 2003; Shah et al., 2008), and adsorbents for heavy metals (Bensacia et al., 2014; Mureseanu et al., 2010; Sierra and Perez-Quintanilla, 2013).

It is well known that heavy metals are major pollutants of wastewaters and have become a major environmental issue due to their toxicity. Heavy metals are not biodegradable and tend to accumulate in living organisms (Bensacia et al., 2014; Gerçel and Gerçel, 2007; Júnior et al., 2009; Mureseanu et al., 2008). Many heavy metal ions are known to be toxic or carcinogenic. Of the hazardous metals, cadmium is considered very toxic. Higher levels of cadmium intake causes malfunction of the kidneys, spilling proteins in the urine and disrupting protein metabolism (Patterson and Passino, 1987; Srivastava et al., 2006). Several harmful effects have been attributed to cadmium in living systems, e.g. isomorphic substitution of cadmium (fragilization of bone tissues) (Forstner and Wittmann, 1981). Moreover, potable water is essential for the human existence and the ecosystem. The removal of hazardous substances from different waters has been widely studied (Bulgariu et al., 2010; Georgescu et al., 2013; Hlihor et al., 2013; Hristodor et al., 2010; Koubaissy et al., 2011; Moulay et al., 2013; Ofomaja et al., 2010; Shahbazi et al., 2011; Vasudevan et al., 2010). Therefore, eliminating the heavy metal ions from water and wastewater has become a challenge for researchers (Moulay et al., 2013; Mureseanu et al., 2008, 2010).

Various techniques have been employed to remove metal ions from aqueous solutions, such as ion-exchange, reverse osmosis, membrane filtration, evaporative recovery, phytoextraction, conventional coagulation, precipitation, sedimentation, electro-dialysis, electrochemical treatments and adsorption (Rousseau, 1987). Still, adsorption is considered more appropriate for removing heavy metals. Indeed, the adsorption process offers a flexible design and operation, and generally yields high-quality treated effluents. In addition, because adsorption is sometimes reversible, the adsorbents can be recovered via relevant desorption processes.

Various sorbents have been valorized in the removal of heavy metals from aqueous solutions (Bensacia and Moulay, 2012; Khelifa et al., 2013; Olu-Owolabi and Unuabonah, 2010; Unuabonah et al., 2007), but the demand to develop novel and high-efficiency adsorbents is ever growing. The use of materials with chemically functionalized surface, such as functionalized mesoporous materials shows improved selectivity for the removal of heavy metals in wastewater. Several studies were reported using mercapto and amino groups, but few cases dealt with carboxylic groups (Bruzzoniti et al., 2007; Rosenholm et al., 2007; Yang et al., 2004; Xu et al., 2008). From the standpoint of green chemistry, the development of environmentally safer solids would be desirable. In this context, TUD-1, three-dimensional mesoporous silica, was first described in 2000 (Jansen et al., 2001). The surfactant-free synthesis of TUD-1 makes it environmentally friendly. Introducing organic groups by grafting organosiloxane precursors to the pore surface yields functional mesoporous hybrid materials with improved thermal, mechanical and chemical stabilities.

Mesoporous hybrid materials are promising adsorbents for removing heavy metals from aqueous solutions. According to a literature survey, there are no studies on the Cd^{2+} adsorption to COOH/TUD-1. Therefore, the objective of the current work is to investigate the adsorption properties of the COOH/TUD-1 towards Cd^{2+}. Adsorption is a very complex process, and its characteristics were evaluated as a function of the process variables such as pH, contact time and temperature. Equilibrium data were examined using Langmuir, Freundlich and Temkin isotherm models. The adsorption mechanism was also investigated in terms of its thermodynamics and kinetics.

2. Experimental

2.1. Reagents and materials

Tetraethylorthosilicate (TEOS, 98%) and triethanolamine (TEA, 97%) were supplied by Acros, and tetraethyl ammonium hydroxide (TEAOH, 35%) by Sigma-Aldrich. 4—(Triethoxysilyl)butyronitrile, ($(EtO)_3Si$-BuCN, 97%)), the grafting agent, was purchased from Sigma-Aldrich. All chemicals and solvents were used as received. Milli-Q deionized water was used for all experiments.

2.2. Synthesis of mesoporous TUD-1

The TUD-1 sample was synthesized following the hydrothermal method (Jansen et al., 2001; Quek et al., 2009), using TEA and TEOS as template and silica precursor, respectively. The gel was prepared as follows: the TEA was added to distilled water and drop wise to TEOS. The resulting mixture was blended using a magnetic stirrer for 60 min and then added to the TEAOH.

The obtained gel was aged for 24 h at room temperature, transferred to a stainless steel Teflon-lined autoclave and heated under static conditions. After 10 h at 180 °C, the mesoporous solid was calcined at 600 °C for 10 h in air to remove the template.

2.3. COOH/TUD-1: Preparation via grafting procedure

First, excess water was removed from the pores of 3 g of mesoporous TUD-1 by drying at 110 °C for 12 h. Then, the sample was dispersed in 200 mL of toluene via ultrasonic stirring, and the necessary quantity of $(EtO)_3Si$-BuCN was added at room temperature under argon with stirring for 24 h. The grafting reaction was performed under argon while refluxing in toluene for 24 h. The resulting precipitate, CN/TUD-1, was then washed in a Soxhlet apparatus with toluene (2 h) and then ethanol for 24 h. This washing was followed by heat treatment at 60 °C for 12 h under vacuum ($<10^{-2}$ bar). The CN/TUD-1 was acidified with H_2SO_4 for 24 h at 90 °C to afford the COOH/TUD-1.

2.4. Characterization methods

2.4.1. N_2 adsorption-desorption isotherms (BET method)

The textural properties of the mesoporous matrices were determined from the nitrogen sorption isotherms recorded at -196 °C using a Micromeritics TriStar apparatus. The total pore volume was estimated from the amount of nitrogen adsorbed at a relative pressure of 0.99.

The pore size distributions were calculated from the adsorption and desorption branches of the corresponding nitrogen isotherm via the Barrett-Joyner-Halenda (BJH) method. The specific area of the samples were calculated via the standard BET procedure using the nitrogen adsorption data collected at a relative equilibrium pressure interval. Before the adsorption experiments, each sample was dried at 150 °C for 15 h under vacuum to ensure a clean and dry surface, and free of any loosely adsorbed species.

2.4.2. X-ray diffraction (XRD)

The XRD patterns were recorded using a Bruker D8 powder diffraction system with a CuKα radiation source (λ = 1.54 Å). The diffraction patterns were collected under ambient conditions over the low angle ranges from 0.5-6°.

2.4.3. Transmission electron microscopy (TEM)

A TEM study of non- and carboxyl-functionalized TUD-1 samples was performed using a TopCon 2100 FCs microscope operating at 200 kV with very low illumination to avoid destroying the material with the electron beam. The samples were crushed and dispersed ultrasonically in acetone at room temperature and spread onto a perforated carbon-copper microgrid.

2.4.4. Fourier transform infrared (FT-IR)

The FT-IR spectra of the mesoporous carboxyl-functionalized adsorbents COOH/TUD-1 were recorded using a Digilab Excalibur 3000 instrument with 128 scans in the mid-IR (4000-400 cm^{-1}) region by means of the KBr pellet technique.

2.5. Heavy metal adsorption experiments

The adsorption of Cd^{2+} by the functionalized and non-functionalized mesoporous TUD-1 was studied using batch experiments. We investigated the effects of contact time, solution pH and temperature.

These batch sorption experiments were performed in a shaking incubator at 150 rpm for 2 h using capped 50 mL-plastic centrifuge tubes containing 0.01 g/L Cd^{2+} solutions and 0.02 g of the adsorbents. The solution pH was adjusted using 0.1 mol/L HCl or NaOH. All of these experiments were replicated four times, and the average results are presented. The extent of adsorbed metal ion (A) was calculated using Eq. (1):

$$A(\%) = \frac{c_0 - c_e}{c_0} \times 100 \quad (1)$$

mesoporous material was calculated using Eq. (2):

$$q_e = \frac{V(c_0 - c_e)}{w} \quad (2)$$

where C_0 and C_e represent the initial and equilibrium metal ion concentrations (g. L^{-1}), respectively, V the metal ion solution volume (L), and w the amount of adsorbent (g).

3. Results and discussion

3.1. Preparation and characterization of TUD-1 and COOH/TUD-1

Three silanol groups exist on the ordered nanoporous silica surface (Fig. 1). They are free, hydrogen-bonded hydroxyl and geminal groups, free and geminal silanol groups being the only chemically reactive ones. The types and number of these silanol groups depend on the way the template was removed and the post-treatment process (Zhao et al., 1997).

To preserve the free and geminal silanol groups, the treatment of the catalysts is very crucial. The sample pores were freed via an extraction/calcination followed by an alcohol treatment before the grafting procedure in order to maintain the free and germinal silanol groups. Furthermore, nitrile functional groups (CN) were covalently incorporated into the nanoporous silica via a post-grafting strategy. These CN groups were hydrolyzed using H_2SO_4 to generate COOH. The grafting procedure was confirmed by several physico-chemical techniques.

3.2. Water stability of 10 wt.% COOH/TUD-1 materials

Stability towards water is an important propriety of porous materials. A 10 wt.% COOH/TUD-1 sample was tested in water at a temperature of 100°C and an agitation speed of 300 rpm for 12, 24, 150 and 300 h, and the results were monitored via low angle XRD (Fig. 2).

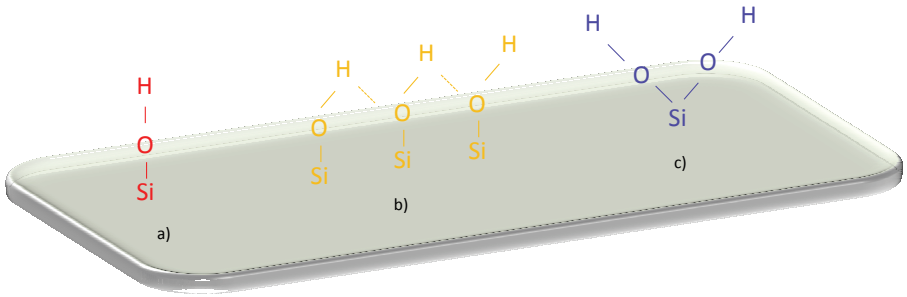

Fig. 1. Illustration of the three silanol groups on mesoporous silica: free (a), hydrogen-bonded hydroxyl (b) and geminal (c)

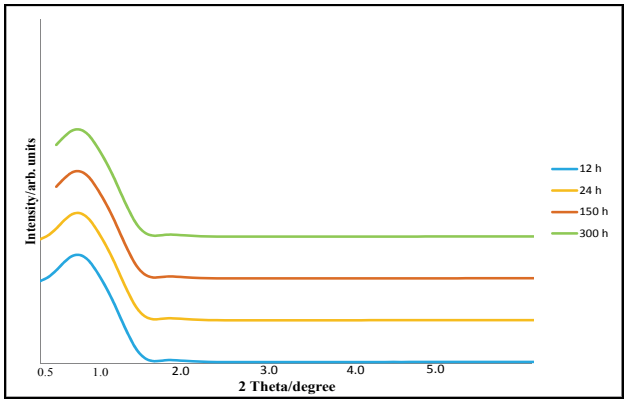

Fig. 2. Low angle XRD patterns of 10 wt.% COOH/TUD-1

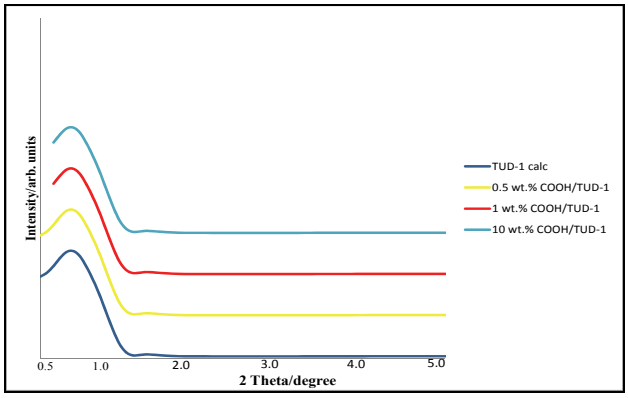

Fig. 3. Low angle XRD patterns of TUD-1 and COOH/TUD-1

No change in the BET surface area was observed (Table 1). Notably, no sample degradation occurred in these conditions, suggesting that the 10 wt.% COOH/TUD-1 sample presents excellent stability.

3.3. Physico-chemical characterization

The XRD measurements were performed to ascertain the changes in the structure of the TUD-1 after grafting procedure. The XRD patterns at low angles for the parent and grafted TUD-1 samples are shown in Fig. 3. This Figure shows a single diffraction peak at low angles of 0.7-0.8°, indicating that the TUD-1 samples are amorphous mesostructured materials (Haddoum et al., 2012; Maschmeyer and Aquino, 2009). These results would indicate that the long-range structural order was maintained for the COOH/TUD-1 materials. These XRD patterns coincide well with data reported in the literature (Haddoum et al., 2012).The BET specific surface areas and pore distributions for the TUD-1 and COOH/TUD-1 adsorbents are presented in Table 1. These results confirmed the mesoporous nature of all samples and indicated that the mesoporous structure was retained after grafting procedure. However, it must be noted that the introduced carboxylic groups decreased the surface area (S_{BET}), the pore diameter (D_p), and the pore volume (V_p) (Table 1).

The TEM images (Fig. 4) show a fully disordered sponge-like or wormhole mesoporous structure with a three-dimensional regular pore structure.

These results suggest that the TUD-1 mesostructure was not destroyed for any sample and remained unaffected after incorporating the carboxylic groups via post-grafting procedure. These TEM images of the grafting samples showed a structure comparable to that of pure TUD-1 mesoporous materials (Jansen et al., 2001).

The IR spectrum of 10 wt.% COOH/TUD-1 is shown in Fig. 5. No vibrations from the original CN groups were observed. The peaks attributed to the carboxyl groups were obvious at 1721 cm^{-1} (stretching of C=O bond), 1415 cm^{-1} (bending of O–H bond), 1282 cm^{-1} (stretching of C–O bond), and 897 cm^{-1} (bending of O–H bond).

3.4. Heavy metal adsorption studies

The pH has a significant effect on the amount of immobilized metal ions, probably related to the degree of protonation of the binding sites on the polyampholyte surface. It is relevant herein to mention that Cd species exist in the forms of Cd^{2+}, $Cd(OH)^{+}$, $Cd(OH)_2°$, $Cd(OH)_3^{-}$ at different pH values (Copello et al., 2012).

The removal of Cd^{2+} was investigated over a pH range from 2 to 7, at 25 °C as shown in Fig. 6. This figure indicates that the Cd^{2+} uptake is pH-dependent. A pH of 2.0 yielded a poor adsorption performance; COOH/TUD-1 adsorbed less Cd^{2+} (3.0%) onto its surface adsorption sites.

Table 1. Textural properties of the mesoporous TUD-1 samples

Sample	S_{BET} ($m^2 . g^{-1}$)	D_p (nm)	V_p ($cm^3 . g^{-1}$)
TUD-1	620	7.3	0.98
0.5 wt.% COOH/TUD-1	620	7.3	0.98
1.0 wt.% COOH/TUD-1	586	6.9	0.81
10 wt.% COOH/ TUD-1	348	5.6	0.54
10 wt.% COOH/ TUD-1 (12 h)	348	5.6	0.54
10 wt.% COOH/ TUD-1 (24 h)	348	5.6	0.54
10 wt.% COOH/ TUD-1 (150 h)	348	5.6	0.54
10 wt.% COOH/ TUD-1 (300 h)	348	5.6	0.54

Notes:10 wt.% COOH/ TUD-1 (12 h) : 10 wt.% COOH/TUD-1 sample tested in water for 12 h;10 wt.% COOH/ TUD-1 (24 h) : 10 wt.% COOH/TUD-1 sample tested in water for 24 h; 10 wt.% COOH/ TUD-1 (150 h) : 10 wt.% COOH/TUD-1 sample tested in water for 150 h; 10 wt.% COOH/ TUD-1 (300 h) : 10 wt.% COOH/TUD-1 sample tested in water for 300 h

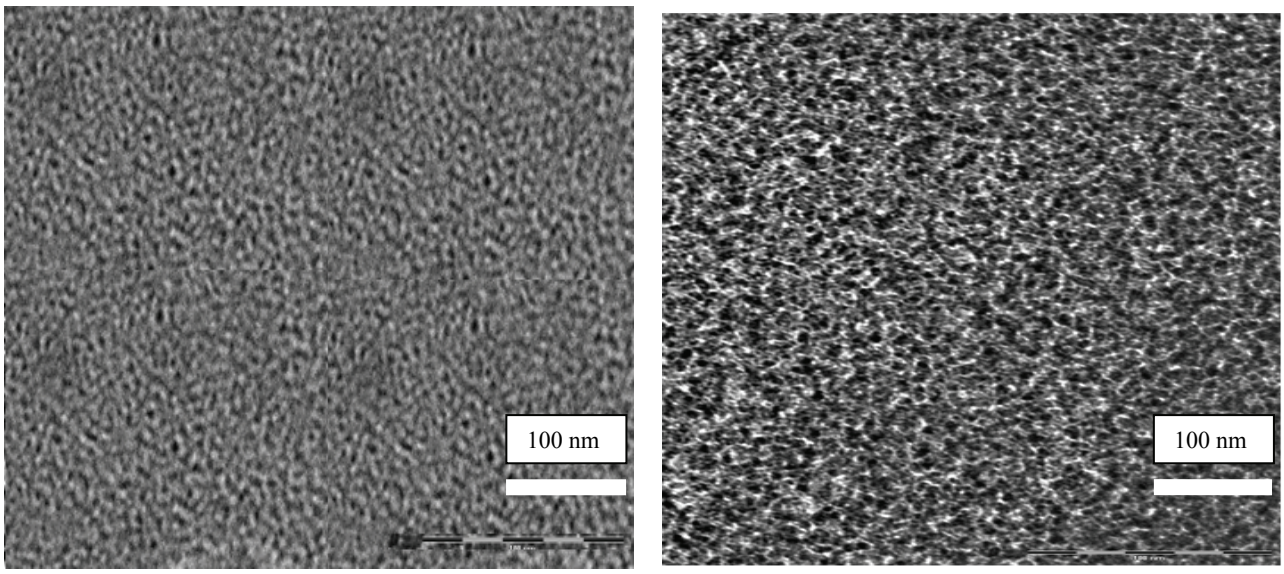

(A) **(B)**

Fig. 4. TEM micrographs of TUD-1 **(A)** and 10 wt.% COOH/TUD-1 **(B)**

The Cd^{2+} removal efficiency increased remarkably as the solution pH increased from 2 to 5.5, then increased slowly with further increases in pH or almost keeps constant. In this case, increasing the solution pH weakened the complexation and more Cd was adsorbed by the COOH/TUD-1.

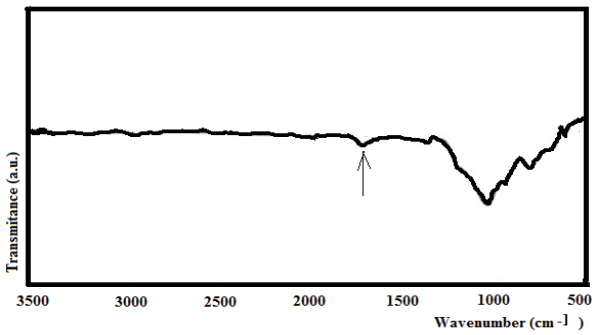

Fig. 5. IR-spectrum of 10 wt.% COOH/TUD-1 sample

The ions exchange interaction exists between the COOH/TUD-1 and Cd ions which favors adsorption. At pH < 7, the Cd species is Cd^{2+} or $Cd(OH)^{+}$ and the removal of Cd is accomplished by sorption. To ensure a quantitative adsorption and avoid metal ion hydrolysis at higher pH values, the pH of 6 was chosen as the optimum for these studies.

The effect of time (from 0 to 500 min) on the Cd^{2+} sorption was determined by equilibrating the TUD-1-sorbate aliquot of pH 6 at 25, 30 and 35 °C (Fig. 7). The non-functionalized TUD-1 showed no propensity to retain the Cd ions (Fig. 7), hinting at the importance of the COOH functional groups. The efficiency of 10 wt.% COOH/TUD-1 for removing Cd^{2+} from solution was determined from the Cd^{2+} adsorption rate, which may be associated with the wastewater cleanup efficiency.

The adsorption rate curve indicates that the Cd^{2+} adsorption was rapid during the first 15 min and nearly complete by 35 min with ca.80-90% of the total Cd^{2+} having been adsorbed at all temperatures. Increasing the contact time further yielded no further adsorption. The 10 wt.% COOH/TUD-1 sample clearly exhibited rapid kinetics for Cd^{2+} removal form an aqueous solution with a saturation time of 35 min. Such behavior of this adsorbent may be explained by the presence of numerous vacant sites homogeneously distributed throughout its surface and

within its inner porous structure. These sites were available for adsorption during the initial stages, which led to the rapid Cd^{2+} uptake increase.

Because the sites have a high affinity for Cd^{2+}, these ions can easily reach these adsorption sites where they are trapped, and rapidly filled them. Although the time required for rapid equilibrium was found to be 40 min, a contact time of 80 min was used for the remaining studies. As shown in Fig. 7, the adsorption capacity was not significantly affected by temperatures higher than 25 °C, a chosen temperature for the remaining experiments.

To evaluate and optimize the adsorption behavior (Ofomaja et al., 2010), we used the coefficient of determination, r^2. The linear coefficient of determination was calculated from the sum of the square of X (S_{xx}), the sum of the square of Y (S_{yy}) and the sum of the square of XY (S_{xy}) as represented by the Eqs. (3-6):

$$r^2 = S_{xy}^2 \Big/ S_{xx} S_{yy} \quad (3)$$

$$S_{xx} = \sum_{i=1}^{n} x_i^2 - \left(\sum_{i=1}^{n} X_i \right) \Big/ n \quad (4)$$

$$S_{yy} = \sum_{i=1}^{n} y_i^2 - \left(\sum_{i=1}^{n} Y_i \right) \Big/ n \quad (5)$$

$$S_{xy} = \sum_{i=1}^{n} X_i y_i^2 - \left(\sum_{i=1}^{n} X_i \right) \left(\sum_{i=1}^{n} y_i \right) \Big/ n \quad (6)$$

These values may vary from 0 to 1. When the coefficient of determination is 1, 100% of the variation in adsorption capacity has been explained by the regression equation.

The model efficiency, *E* (Olu-Owolabi and Unuabonah, 2010), was calculated by Eq. (7):

$$E = 1 - \frac{\sum_{i=1}^{N} w_i \left(S_i - \hat{S}_i \right)^2}{\sum_{i=1}^{N} \left(S_i - \hat{S}_{wavg} \right)^2} \quad (7)$$

where $\hat{S}_{wavg}$ is the weighted mean of the measured values.

This statistical measure is considered by many to be the best overall indicator of model fit because it has good resistance to errors due to extreme experimental values (Olu-Owolabi and Unuabonah, 2010). A model efficiency-*E* of *1* indicates a perfect fit to the data, whereas an $E < 0$ indicates that averaging the measured values yields better predictions than the model.

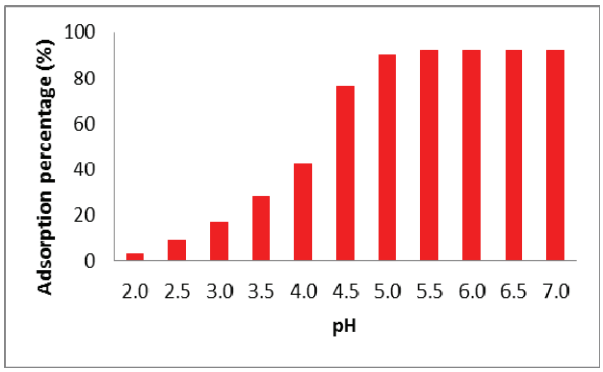

Fig. 6. Effect of pH on Cd(II) adsorption

3.4.1. Adsorption kinetics

Adsorption kinetics are essential for wastewater treatment because they provide the necessary information on the reaction pathway and adsorption dynamics.

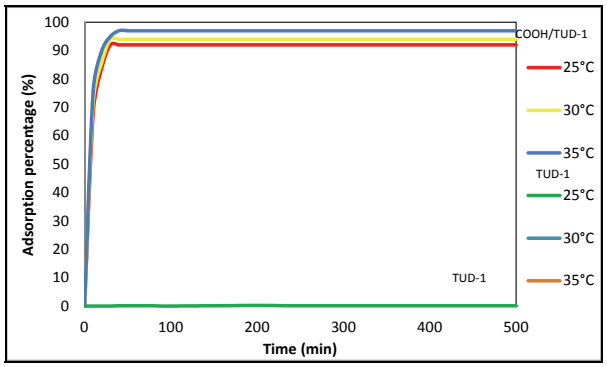

Fig. 7. Influence of the contact time and temperature on the Cd^{2+} adsorption by TUD-1 and 10 wt.% COOH/TUD-1 at pH 6

The sorption behavior for Cd ions on 10 wt.% COOH/TUD-1 was confirmed using the Lagergren pseudo-first order and chemisorption pseudo-second order kinetic models.

3.4.1.1. Pseudo-first-order model

Lagergren (1898) showed that the adsorption rate of a solute on an adsorbent is based on the adsorption capacity. The pseudo-first-order rate expression is represented by the differential law (Eq. 8):

$$dq_t / dt = k_1 (q_e - q_t) \quad (8)$$

k_1 is the pseudo-first-order rate constant; q_e is the adsorption capacity of the adsorbent (mg. g^{-1}); q_t is the amount of Cd ion adsorbed at time *t* (mg. g^{-1}).

By integrating for $t = 0$ to $t = t$ and $q_t = 0$ to $q_t = q_t$, the following linear expression can be obtained (Eq. 9):

$$\log(q_e - q_t) = \log q_e - k_1 t / 2.303 \quad (9)$$

where k_1 is computed from the slope of the plot of $\log(q_e - q_t)$ versus *t* (Fig. 8).

3.4.1.2. Pseudo-second-order kinetic model

The pseudo-second-order reaction is greatly affected by the amount of metal on the adsorbent surface at equilibrium. This rate is directly proportional to the number of active surface sites. Huo (Ho and McKay, 1999) developed a pseudo-second-order kinetic expression for the sorption system of divalent metal ions (Eqs. 10-13), which we used to investigate the adsorption mechanism and rate constants for adsorbing Cd^{2+} to 10 wt.% COOH/TUD-1 (Fig. 9).

$$q_t = kq_e^2 t \tag{10}$$

$$dq_t/dt = k(q_e - q_t)^2 / (1 + kt) \tag{11}$$

$$1/(q_e - q_t) = kt + 1/q_e \tag{12}$$

$$1/q_t = 1/q_e + 1/kq_e^2 \tag{13}$$

k is the rate constant of the pseudo-second order equation.

The pseudo-first-order and pseudo-second-order sorption kinetic parameters are shown in Table 2. The correlation coefficients for the pseudo-second-order model are much higher than for the pseudo-first-order model.

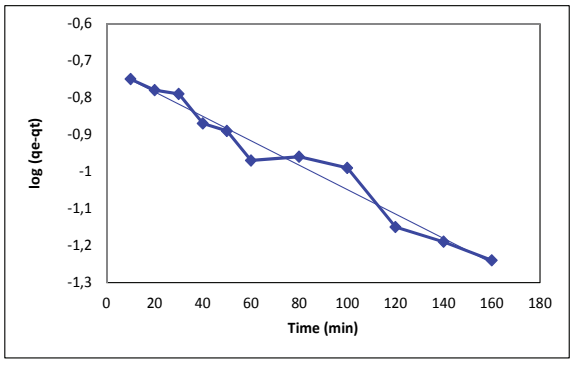

Fig. 8. Pseudo-first-order model fit for the adsorption of Cd^{2+} onto 10 wt.% COOH/TUD-1

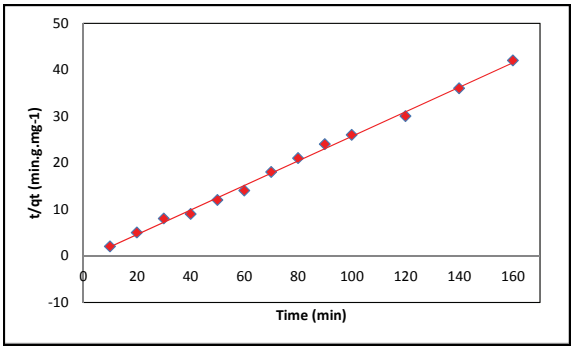

Fig. 9. Pseudo-second order model fit for the adsorption of Cd^{2+} onto 10 wt.% COOH/TUD-1

Therefore, the experimental values of *qe* do not agree well with the calculated theoretical values. Thus, the sorption mechanism of the Cd^{2+} ion onto 10 wt.% COOH/TUD-1 does not follow the pseudo-first-order kinetics model. The adsorbent system is described well by the pseudo-second-order kinetics model, which implies that the adsorption of Cd^{2+} onto COOH/TUD-1 may occur via a chemical process involving valence forces that share or exchange electrons.

3.4.2. Adsorption isotherms

The adsorption isotherm indicates how the adsorbed molecules are distributed between the liquid and solid phases when the adsorption process reaches equilibrium. Analyzing the isotherm data by fitting them to different models is important to determine which model is suitable for design purposes. In this study, the equilibrium experimental data for Cd^{2+} ions adsorbed onto the COOH/TUD-1 beads were analyzed using the Langmuir, Freundlich and Temkin models.

3.4.2.1. Langmuir isotherm model

The Langmuir equation may be written as follows (Eq. 14):

$$q_e = (Q_{max} K_L C_e)/(1 + K_L C_e) \tag{14}$$

The expression for the linear form of Langmuir isotherm is as follows (Eq. 15):

$$C_e/q_e = (1/Q_{max} K_L) + (C_e/Q_{max}) \tag{15}$$

where q_e is the equilibrium capacity of Cd (II) per unit weight of the adsorbent (mg/g), Q_{max} is the maximum adsorption capacity of the adsorbent corresponding to complete monolayer coverage on the surface (mg. g^{-1}), K_L - the Langmuir adsorption constant related to the energy of adsorption (L. mg^{-1}), C_e - the equilibrium concentration of the solute in the bulk solution (mg. L^{-1}).

The constant Q_{max} and K_L can be calculated from the intercepts and the slopes of the linear plots of C_e/q_e versus C_e. These parameters were obtained with the linear fitting procedure and are listed in Table 2.

The Langmuir model (Langmuir, 1916) assumes a monomolecular layer formation when adsorption takes place without any interactions between the adsorbed molecules. All of the adsorption sites on the surface involved are assumed to be energetically identical with no transmigration of the sorbate across the solid sorbent surface. In such cases, the intermolecular forces decrease as the distance from the adsorption surface increases.

3.4.2.2. Freundlich isotherm model

The Freundlich model (Adamson and Gast, 1997; Freundlich, 1906) is a commonly used model for analyzing adsorption data. The Freundlich model equation may be written as follows (Eq. 16):

$$q_e = K_F C_e^{1/n} \tag{16}$$

A linear form of the Freundlich expression can be obtained by taking logarithms (Eq. 17).

$$\log q_e = \log K_F + (1/n)\log C_e \quad (17)$$

where q_e is the amount of solute adsorbed per unit weight of adsorbent (mg. g^{-1}), K_F - the Freundlich constant indicating the relative adsorption capacity for the adsorbent (mg. g^{-1}), C_e - the equilibrium concentration of the solute in the bulk solution (mg. L^{-1}), 1/n the heterogeneity factor indicating the adsorption intensity.

Freundlich isotherm theory states that the ratio of solute adsorbed onto a given mass of sorbent to the solute concentration in solution is not constant over different concentrations. This model is based on the relation between the adsorbed quantity and solute concentration at equilibrium. It describes non-ideal and reversible adsorption and is not restricted to a monolayer.

This empirical model can be applied to multilayer adsorptions, with a non-uniform distribution for adsorption heat and affinity over a heterogeneous surface.

3.4.2.3. Temkin isotherm model

Temkin isotherm model is the early model describing the adsorption of hydrogen onto platinum electrodes within the acidic solutions.

The Temkin model equation may be written as follows (Eq. 18):

$$q_e = (RT/b)ln(AC_e) \quad (18)$$

A linear form of the Temkin expression may be written as follows (Eq. 19):

$$q_e = B\,ln\,A + B\,ln\,C_e \quad (19)$$

where $B = RT/b$, b - the Temkin constant related to heat of sorption (J. mol^{-1}); A - the Temkin isotherm constant (L.g^{-1}); R - the gas constant 8.314 J/mol. K; T - the absolute temperature (K).

The constants A and B are drawn from the intercept and slope of the plot, respectively, and are listed in Table 2.

The Temkin isotherm (Temkin and Pyzhev, 1940a) comprises a factor that takes into account the adsorbent-adsorbate interactions. Moreover, Temkin and Pyzhev considered the effects of indirect adsorbate/adsorbate interaction on adsorption isotherms and suggested that, because of these interactions, the heat of adsorption of all the molecules in the layer would decrease linearly rather than logarithmic with coverage (Aharoni and Ungarish, 1977; Temkin and Pyzhev, 1940b). Temkin equation is excellent for predicting the gas phase equilibrium (when organization in a tightly packed structure with identical orientation is not necessary).

Our results for the COOH/TUD-1 are gathered in Table 2. The Langmuir, Freundlich and Temkin isotherm parameters and correlation coefficients are summarized. The coefficient of determination (r^2) was found to be 0.9989, 0.9702, and 0.7327 for Langmuir model, Freundlich's and Temkin's, respectively.

These results indicate that the Cd^{2+} adsorption to COOH/TUD-1 fitted the Langmuir model better than the Freundlich's and the Temkin's, which may be due to the homogenous distribution of active sites on the COOH/TUD-1 surface because the Langmuir equation assumes a homogenous surface where all sites have equal adsorption energies. The 1/n values were between 0 and 1, which indicates that the Cd^{2+} adsorption to COOH/TUD-1 was favorable under the studied experimental conditions.

3.4.3. Thermodynamic adsorption parameters

To understand the adsorption process and the solute distribution between the sorbent solid and the liquid phases for Cd^{2+} on mesoporous COOH/TUD-1, assessing the thermodynamic parameters is important. The Gibbs free energy *(ΔG°),* the change in entropy *(ΔS°),* and the change in enthalpy (ΔH°) are calculated (Adebowale et al., 2008; Atar et al., 2012; Olu-Owalbi et al., 2012; Young and Crowell, 1962) using the following equations (Eqs. 20-25):

Table 2. Adsorption parameters of 10 wt.% COOH/TUD-1

Pseudo-first-order	*Pseudo-second-order*	*Langmuir model*	*Freundlich model*	*Temkin model*	*Thermodynamic parameters*	*Adsorption (%)*	*Desorption (%)*
q_e, exp. = 3.15 (mg.g^{-1})	q_e, exp. = 3.15 (mg.g^{-1})				ΔG^0 (J. mol^{-1}) = -6295	90	100
q_e, calc. = 0.27	q_e, calc. =3.21	q_{max} (mg.g^{-1}) = 72.34	n = 2.52	A = 68.92	ΔH^0 (J. mol^{-1}) = 3703.63	90	98
k_1 = 0.0116	k_2 = 0.1006	K_L (L mg^{-1}) = 0.03331	K_F = 7.23	B = 5.02	ΔS^0 (J. mol^{-1} K^{-1}) = 32.93	90	98 (after 10 times)
r^2 = 0.9703	r^2 = 0.9989	r^2 = 0.9989	r^2 = 0.9702	r^2 = 0.7327	r^2 = 0.9889	r^2 = 0.9976	r^2 = 0.9836
E^2 = 0.9715	E^2 = 0.9979	E^2 = 0.9990	E^2 = 0.9802	E^2 = 0.8345	E^2 = 0.9982	E^2 = 0.9987	E^2 = 0.9947

exp. – experimental; calc. – calculated

$$\Delta G = -RT \ln K \quad (20)$$

$$K = \frac{c_0 - c_e}{c_e}\frac{V}{w} \quad (21)$$

$$\ln K = \frac{\Delta S^0}{R} - \frac{\Delta H^0}{RT} \quad (22)$$

$$\frac{d \ln C_e}{dt} = \frac{\Delta H}{RT^2} \quad (23)$$

$$\Delta H = -R\left[\frac{d(\ln C_e)}{d(1/T)}\right] \quad (24)$$

$$\Delta G^0 = \Delta H^0 - T\Delta S^0 \quad (25)$$

where $\Delta G°$ - the changes in free energy ($Jmol^{-1}$), R - the ideal gas constant (8.314 $Jmol^{-1}K^{-1}$), T - the absolute temperature (K), K - the equilibrium constant, C_e - the equilibrium metal ion concentration (mgL^{-1}).

Besides the degree of spontaneity for the adsorption process, the higher negative values of Gibbs free energy indicate a more energetically favorable adsorption. In our study, the calculated Gibbs energy was negative (Table 2), suggesting a thermodynamically spontaneous adsorption process of Cd^{2+} onto COOH/TUD-1.

The changes in enthalpy *(ΔH°)* and entropy *(ΔS°)* were calculated from the slopes and intercepts of a plot of *lnK* vs. *1/T*, respectively. The plots were not given but the results are shown in Table 2. The calculated enthalpy of the adsorption, ΔH°, is positive in aqueous solution, which indicates that the adsorption of metal ions is an endothermic process. Because the enthalpy of adsorption is a measurement of the energy barrier (which must be overcome by the reacting molecules) (Jencks, 1969), these results suggest that the heat is consumed upon the transfer occurrence of the metal ions from the aqueous to the solid phase.

ΔS° can be used to identify whether the adsorption reaction follows an associative or dissociative mechanism. Generally, a change in entropy of $\Delta S° > -10$ $Jmol^{-1}K^{-1}$ implies a dissociative mechanism (Scheckel and Donald, 2001; Zhao et al., 2011). In this work, the standard entropy change for the adsorption system (ΔS°) was positive (Table 2). This result reveals that the Cd^{2+} adsorption onto the adsorbents produced a less ordered molecular arrangement (Zhao et al., 2011). Therefore, the distribution of rotational and translational energy for a small number of molecules on the COOH/TUD-1 increases with increasing adsorption because of the positive $\Delta S°$, and this randomness increases at the COOH/TUD-1 solid - Cd solution interface during the adsorption process. The entropy changes were all positive, which implies that a dissociative mechanism was involved in the adsorption processes.

3.4.4. Desorption efficiency

Recovery is important to the mesoporous sorbent quality. The reversibility of Cd^{2+} adsorption to COOH/TUD-1 was studied and the results and procedure are compiled in Table 2. Cd^{2+} ions adsorbed to COOH/TUD-1 were effectively eluted with HCl aqueous solutions. The highest recovery was found to be 98% using 1 M HCl.

The results for the adsorption-desorption cycle demonstrated COOH/TUD-1 could be re-used up to 10 times without significantly changing the adsorption extent of the studied metal ions. Therefore, the prospects of COOH/TUD-1 are promising in the applications for removing Cd^{2+} from water and wastewater.

4. Conclusions

The ordered functionalized mesoporous silica COOH/TUD-1, used to remove Cd^{2+} from polluted water, was prepared via a post-grafting pathway and characterized using several physicochemical techniques. The ability of COOH/TUD-1 to remove Cd^{2+} ions from aqueous solutions was analyzed via a batch technique. The optimum pH value for Cd^{2+} removal was 6.

The adsorption of Cd to COOH/TUD-1 reached equilibrium within 35 min. The high r^2 values indicate that the Cd adsorption to COOH/TUD-1 follows a pseudo-second-order kinetics model based on the assumption that the rate limiting step may be chemisorption.

The Langmuir, Temkin and Freundlich isotherm models for Cd^{2+} adsorption to COOH/TUD-1 were studied, and the Langmuir model best fit the adsorption data.

The negative value of $\Delta G°$ indicates the feasibility and spontaneity of the adsorption process. The positive value of $\Delta S°$ reflects the affinity of COOH/TUD-1 towards Cd. The positive $\Delta H°$ suggests the endothermal nature of adsorption. Cd adsorption is reversible and can be desorbed from COOH/TUD-1. COOH/TUD-1 can be viewed as a new material for removing toxic metals from wastewater with high efficiency that can be economically regenerated while maintaining its high adsorption capacity.

Acknowledgements

O. Ersen is acknowledged for the kind assistance with the TEM experiments. We thank the Minister of Defense of Algeria and ICPEES Strasbourg France for their financial support.

References

Adamson A.W., Gast A.P., (1997), *Physical Chemistry of Surfaces,* 6th Ed. Wiley- Interscience, New York.

Adebowale K.O., Unuabonah E.I., Olu-Owolabi B.I., (2008), Kinetic and thermodynamic aspects of the adsorption of Pb^{2+} and Cd^{2+} ions on tripolyphosphate-modified kaolinite clay, *Chemical Engineering Journal*, **136**, 99-107.

Aharoni C., Ungarish M., (1977), Kinetics of activated chemisorption, Part 2, Theoretical models, *Journal of the Chemical Society, Faraday Transactions 1*, **73**, 456-464.

Atar N., Olgun A., Wang S., (2012), Adsorption of cadmium (II) and zinc (II) on boron enrichment process waste in aqueous solutions: Batch and fixed-bed system studies, *Chemical Engineering Journal*, **192**, 1-7.

Beck J.S., Vartuli J.C., (1996), Recent advances in the synthesis, characterization and applications of mesoporous molecular sieves, *Current Opinion in Solid State Materials Science*, **1**, 76–87.

Beck J.S., Vartuli J.C., Roth W.J., Leonowicz M.E., Kresge C.T., Schmitt K.D., Chu C.T.W., Olson D.H., Sheppard E.W., McCullen S.B., Higgins J.B., Schlenker J.L., (1992), A new family of mesoporous molecular sieves prepared with liquid crystal templates, *Journal of American Chemical Society*, **114,** 10834–10843.

Bensacia N., Moulay S., (2012), Functionalization of polyacrylic acid with tetrahydroxybenzene via a homolitic patway. Application to metallic adsorption, *International Journal of Polymeric Materials and Polymeric Biomaterials*, **61**, 699-722.

Bensacia N., Fechete I., Moulay S., Hulea O., Boos A., Garin F., (2014), Kinetic and equilibrium studies of lead (II) adsorption from aqueous media by KIT-6 mesoporous silica functionalized with –COOH, *Comptes Rendus Chimie,* **17**, 869-880.

Bernal C., Mesa M., Jaber M., Guth J. L., Sierra L., (2012), Contribution to the understanding of the formation mechanism of bimodal mesoporous MCM41-type silica with large defect cavities, *Microporous and Mesoporous Materials*, **153**, 217-226.

Boulaoued A., Fechete I., Donnio B., Bernard M., Turek P., Garin F., (2012), Mo/KIT-6, Fe/KIT-6 and Mo–Fe/KIT-6 as new types of heterogeneous catalysts for the conversion of MCP, *Microporous Mesoporous Materials*, **155,** 131-142.

Bruzzoniti M.C., Prelle A., Sarzanini C., Onida B., Fiorilli S., Garrone E., (2007), Retention of heavy metal ions on SBA-15 mesoporous silica functionalised with carboxylic groups, *Journal of Separation Science*, **30**, 2414-2420.

Bulgariu L., Ceica A., Lazar L., Cretescu I., Balasanian I., (2010), Equilibrium and kinetics study of nitrate removal from water by purolite A100 Resin, *Roumanian Journal of Chemistry,* **61**, 1136-1141.

Copello G.J., Diaz L.E., Dall'Orto V.C., (2012), Adsorption of Cd(II) and Pb(II) onto a one step-synthesized polyampholyte: Kinetics and equilibrium studies, *Journal of Hazardous Materials*, **217-218**, 374-381.

Da'na E., Sayari A., (2012), Adsorption of heavy metals on amine-functionalized SBA-15 prepared by co-condensation: Applications to real water samples, *Desalination*, **285,** 62–67.

Delacôte C., Gaslain F.O.M., Lebeau B., Walcarius A., (2009), Factors affecting the reactivity of thiol-functionalized mesoporous silica adsorbents toward mercury(II), *Talanta*, **79,** 877–886.

Dumitriu E., Fechete I., Caullet P., Kessler H., Hulea V., Chelaru C., Hulea T., Bourdon X. (2002), Conversion of aromatic hydrocarbons over MCM-22 and MCM-36 catalysts, *Studies in Surface Science and Catalysis,* **142**, 951-958.

Dumitriu E., Secundo F., Patarin J., Fechete I., (2003), Preparation and properties of lipase immobilized on MCM-36 support, *Journal of Molecular Catalysis B: Enzymatic*, **22**, 119-133.

Fechete I., Donnio B., Ersen O., Dintzer T., Djeddi A., Garin F., (2011), Single crystals of mesoporous tungstenosilicate W-MCM-48 molecular sieves for the conversion of methylcyclopentane (MCP), *Applied Surface Science,* **257**, 2791-2800.

Fechete I., Wang Y., Vedrine J.C., (2012a), The past, present and future of heterogeneous catalysis, *Catalysis Today*, **189,** 2-27.

Fechete I., Debbih-Boustila S., Merkache R., Hulea O., Lazar L., Lutic D., Balasanian I., Garin F., (2012b), MnMCM-48, CoMCM-48 and CoMnMCM-48 mesoporous catalysts for the conversion of methylcyclopentane (MCP), *Environmental Engineering and Management Journal*, **11**, 1931-1943.

Fechete I., Ersen O., Garin F., Lazar L., Rach A., (2013), Catalytic behavior of MnMCM-48 and WMnMCM-48 ordered mesoporous catalysts in a reductive environment: a study of the conversion of methylcyclopentane, *Catalysis Science and Technology*, **3**, 444-453.

Forstner U., Wittmann G.T.W, (1981), *Metal Pollution in the Aquatic Environment,* Second Edition, Spring-Verlag, New York, USA.

Freundlich H.M.F., (1906), Over the adsorption in solution*, Journal of Physical Chemistry*, **57**, 385-470.

Ganesan V., Walcarius A., (2008), Ion exchange and ion exchange voltammetry with functionalized mesoporous silica materials, *Materials Science and Engineering B,* **149**, 123–132.

Georgescu I., Mureseanu M., Carja G., Hulea V., (2013), Adsorptive removal of cadmium and copper from water by mesoporous silica functionalized with N-(aminothioxomethyl)-2-thiophen carboxamide, *Journal of Environmental Engineering*, **139**, 1285-1296.

Gerçel Ö., Gerçel H.F., (2007), Adsorption of lead(II) ions from aqueous solutions by activated carbon prepared from biomass plant material of *Euphorbia rigida, Chemical Engineering Journal*, **132**, 289-297.

Haddoum S., Fechete I., Donnio B., Garin F., Lutic D., Chitour C.E., (2012), Fe-TUD-1 for the preferential rupture of the substituted C\C bond of methylcyclopentane (MCP), *Catalysis Communications*, **27**, 141-147.

Hlihor R. M., Diaconu M., Fertu D., Chelaru C., Sandu I., Tavares T., Gavrilescu M., (2013), Bioremediation of Cr(VI) Polluted wastewaters by sorption on heat inactivated saccharomyces cerevisiae biomass, *International Journal of Environmental Research*, **7**, 581-594.

Ho Y.S., McKay G., (1999), Pseudo-second order model for sorption processes, *Process Biochemistry*, **34**, 451-465.

Hristodor C., Copcia V., Lutic D., Popovici E., (2010), Thermodynamics and kinetics of Pb(II) and Hg(II) ions removal from aqueous solution by Romanian clays, *Roumanian Journal of Chemistry*, **61**, 285-289.

Hu B., Liu H., Tao K., Xiong C., Zhou S., (2013), Highly active doped mesoporous KIT-6 catalysts for metathesis of 1-butene and ethene to propene: The

influence of neighboring environment of W species, *Journal of Physical Chemistry C*, **117**, 26385-2639.

Jaber M., Miehé-Brendlé J., Roux M., Dentzer J., Le Dred R., Guth J.L., (2002a), A new Al, Mg-organoclay, *New Journal of Chemistry*, **26**, 1597-1600.

Jaber M., Miehé-Brendlé J., Le Dred R., (2002b), Mercaptopropyl Al-Mg phyllosilicate: Synthesis and characterization by XRD, IR, and NMR, *Chemistry Letters*, **9**, 954-955.

Jansen J.C., Shan Z., Marchese L., Zhou W., van der Puil N., Maschmeyer Th., (2001), A new templating method for three-dimensional mesopore networks, *Journal of the Chemical Society, Chemical Communications*, **8**, 713-714.

Jencks W.P., (1969), *Catalysis in Chemistry and Enzymology,* McGraw-Hill, New York.

Júnior O.K., Gurgel L.V.A., de Freitas R.P., Gil L.F, (2009), Adsorption of Cu(II), Cd(II), and Pb(II) from aqueous single metal solutions by mercerized cellulose and mercerized sugarcane bagasse chemically modified with EDTA dianhydride (EDTAD), *Carbohydrate Polymers*, **77**, 643-650.

Khelifa A., Aoudj S., Moulay S., De Petris-Wery M., (2013), A one-step electrochlorination/electroflotation process for the treatment of heavy metals wastewater in presence of EDTA, *Chemical Engineering and Processing: Process Intensification*, **70**, 110-116.

Koubaissy B., Toufaily J., El-Murr M., Hamieh T., Magnoux P., Joly G., (2011), Elimination of aromatic pollutants present in wastewater by adsorption over zeolites, *Physics Procedia,* **21**, 220-227.

Lagergren S., (1898), For the theory of so-called adsorption of dissolved substances, K. Sven., Vetenskapsakad, Handl, **24**, 1.

Langmuir I., (1916), The constitution and fundamental properties of solids and liquids Part I. Solids, *Journal of American Chemical Society*, **38**, 2221-2295.

Maschmeyer T., Aquino C., (2009), *A New Family of Mesoporous Oxides - Synthesis, Characterizations and Applications of TUD-1,* In: *Ordered Porous Solids: Recent Advances and Prospects,* Valtchev V., Mintova S., Tsapsatis M. (Eds.)*,* Elsevier Science, 3-30.

Moulay S., Bensacia N., Garin F., Fechete I., Boos A., (2013), Polyacrylamide-based sorbents for the removal of hazardous metals, *Adsorption Science and Technology*, **81**, 691-709.

Mureseanu M., Reiss A., Stefanescu I., David E., Parvulescu V., Renard G., Hulea V., (2008), Modified SBA-15 mesoporous silica for heavy metal ions remediation, *Chemosphere*, **73**, 1499-1504.

Mureseanu M., Reiss A., Cioatera N., Trandafir I., Hulea V., (2010), Mesoporous silica functionalized with 1-furoyl thiourea urea for Hg(II) adsorption from aqueous media, *Journal of Hazardous Materials*, **182**, 197-203.

Ofomaja A.E., Unuabonah E.I., Oladoja N.A, (2010), Competitive modeling for the biosorptive removal of copper and lead ions from aqueous solution by Mansonia wood sawdust, *Bioresource Technology*, **101**, 3844-3852.

Olu-Owolabi B.I., Unuabonah E.I., (2010), Kinetic and thermodynamics of the removal of Zn^{2+} and Cu^{2+} from aqueous solution by sulphate and phosphate-modified Bentonite clay, *Journal of Hazardous Materials,* **184**, 731-738.

Olu-Owalbi B.I, Diagboya P.N., Ebaddan W.C., (2012), Mechanism of Pb^{2+} removal from aqueous solution using a nonliving moss biomass, *Chemical Engineering Journal*, **195-196**, 270-275.

Patterson J.W., Passino R., (1987), *Metals Speciation Separation and Recovery,* Lewis Publishers, Chelsea, MA, USA.

Ponomoreva D.A., Yuschenko V.V., Ivanova I.I., Pasqua L., Testa F., Di Renzo F., Fajula F., (2004), Dehydrogenation of ethylbenzene over Ga- and Fe-containing MCM-41, *Studies in Surface Science and Catalysis,* **154**, 2208-2211.

Quek X.Y., Tang Q.H., Hu S.Q., Yang Y.H., (2009), Liquid phase trans-stilbene epoxidation over catalytically active cobalt substituted TUD-1 mesoporous materials (Co-TUD-1) using molecular oxygen, *Applied Catalysis A: General*, **361**, 130-136.

Rosenholm J.M., Czuryszkiewicz T., Kleitz F., Rosenholm J.B., Linden M., (2007), On the nature of the brønsted acidic groups on native and functionalized mesoporous siliceous SBA-15 as studied by benzylamine adsorption from solution, *Langmuir*, **23**, 4315-4323.

Rousseau R.W., (1987), *Handbook of Separation Process Technology,* Wiley, New York.

Sarshar Z., Kleitz F., Kaliaguine S., (2011), Novel oxygen carriers for chemical looping combustion: La 1-xCe xBO_3 (B = Co, Mn) perovskites synthesized by reactive grinding and nanocasting, *Energy and Environmental Science,* **4**, 4258-4269.

Scheckel K.G., Donald L.S., (2001), Temperature effects on nickel sorption kinetics at the mineral–water interface, *Soil Science Society America Journal, 65, 719–728.*

Shah P., Sridevi N., Prabhune A., Ramaswamy V., (2008), Structural features of Penicillin acylase adsorption on APTES functionalized SBA-15**,** *Microporous and Mesoporous Materials***, 116,** 157-165.

Shahbazi A., Younesi H., Badiei A., (2011), Functionalized SBA-15 mesoporous silica by melamine-based dendrimer amines for adsorptive characteristics of Pb(II), Cu(II) and Cd(II) heavy metal ions in batch and fixed bed column, *Chemical Engineering Journal,* **168**, 505-518.

Sierra I., Perez-Quintanilla D., (2013), Heavy metal complexation on hybrid mesoporous silicas: an approach to analytical applications, *Chemical Society Review*, **42**, 3792-3807.

Srivastava V.C., Deo Mall I., Mishra I.M., (2006), Equilibrium modelling of single and binary adsorption of cadmium and nickel onto bagasse fly ash, *Chemical Engineering Journal*, **117**, 79–91.

Staub H., Del Rosal I., Maron L., Kleitz F., Fontaine F.-G., (2012), On the interaction of phosphines with high surface area mesoporous silica, *Journal of Physical Chemistry C*, **116**, 25919-25927..

Temkin M.I., Pyzhev V., (1940a), Kinetics of ammonia synthesis on promoted iron catalyst, *Acta Physico-Chimica USSR*, **12**, 327–356.

Temkin M.J, Pyzhev V., (1940b), Recent modifications to Langmuir isotherms, *Acta Physico- Chimica, USSR*, **12**, 217–222.

Tsoncheva T., Rosenholm J., Linden M., Kleitz F., Tiemann M., Ivanova L., Dimitrov M., Paneva D., Mitov I., Minchev C., (2008), Critical evaluation of the state of iron oxide nanoparticles on different mesoporous silicas prepared by an impregnation method, *Microporous and Mesoporous Materials,* **112**, 327-337.

Tsoncheva T., Issa G., Genova I., Dimitrov M., (2013), Formation of catalytic active sites in copper and

manganese modified SBA-15 mesoporous silica, *Journal of Porous Materials*, **20**, 1361-1369.

Unuabonah E.I., Olu-Owolabi B.I., Adebowale K.O., Ofomaja A.E., (2007), Adsorption of lead and cadmium ions from aqueous solutions by tripolyphosphate-impregnated Kaolinite clay, *Colloids and Surfaces A: Physicochemical and Engineering Aspects*, **292**, 202-211.

Vasudevan S., Epron F., Lakshmi J., Ravichandran S., Mohan S., Sozhan G., (2010), Removal of NO_3^- from Drinking Water by Electrocoagulation – An Alternate Approach, *Clean-Soil, Air, Water,* **38**, 225-229.

Visuvamithiran P., Shanthi K., Palanichamy M., Murugesan V., (2013), Direct synthesis of Mn-Ti-SBA-15 catalyst for the oxidation of ethylbenzene, *Catalysis Science and Technology*, **3**, 2340-2348.

Wu H.-Y., Zhang X.-L., Yang C.-Y., Chen X., Zheng X.-C., (2013), Alkali-hydrothermal synthesis and characterization of W-MCM-41 mesoporous materials with various Si/W molar ratios, *Applied Surface Science*, **270**, 590-595

Xu W., Gao Q., Xu Y., Wu D., Sun Y., Shen W., Deng F., (2008), Controlled drug release from bifunctionalized mesoporous silica, *Journal of Solid State Chemistry*, **181**, 2837-2844.

Yang C., Wang Y., Zibrowius B., Schuth F., (2004), Formation of cyanide-functionalized SBA-15 and its transformation to carboxylate-functionalized SBA-15, *Physical Chemistry Chemistry Physics*, **6**, 2461-2467.

Yen H., Seo Y., Guillet-Nicolas, R., Kaliaguine, S., Kleitz, F., (2011), One-step-impregnation hard templating synthesis of high-surface-area nanostructured mixed metal oxides ($NiFe_2O_4$, $CuFe_2O_4$ and Cu/CeO_2), *Chemical Communications*, **47**, 10473-10475.

Young D.M., Crowell A.D., (1962), *Physical Adsorption of gases, Butterworth, London*, 462.

Zhao X.S., Lu G.Q., Whittaker A.J., Millar G.J., Zhu H.Y., (1997), Comprehensive study of surface chemistry of MCM-41 using ^{29}Si CP/MAS NMR, FTIR, pyridine-TPD, and TGA, *Journal of Physical Chemistry B*, **101,** 6525-6531.

Zhao X., Zhang G., Jia Q., Zhao C., Zhou W., Li W., (2011), Adsorption of Cu(II), Pb(II), Co(II), Ni(II), and Cd(II) from aqueous solution by poly(aryl ether ketone) containing carboxyl groups (PEK-L): Equilibrium, kinetics, and thermodynamics, *Chemical Engineering Journal*, **171**, 152-158.